

Percolation Behaviour in the Magnetic Permeability and Electrical Conductivity in Conducting Magnetic - Insulating Non Magnetic Binary Composites.

David S. McLachlan¹, T B Doyle^{2,3} and Godfrey Sauti⁴.

¹School of Physics, University of the Witwatersrand, Johannesburg, 2050, South Africa.

²Materials Research Division, iTemba LABS, Faure, 7129, South Africa.

³School of Chemistry and Physics, University of KwaZulu-Natal, Durban, 4001, South Africa.

⁴Advanced Materials and Processing Branch, Mail Stop 397, NASA Langley Research Center, Hampton, VA 236891, USA.

Abstract: Experimental results of the complex magnetic permeability (μ) and the electrical conductivity (σ) of a granular paramagnetic Gadolinium Gallium Garnet (GGG: 0.3 to 26 Vol. %) and Teflon (PTFE) system are presented, and discussed in relation to previously published (conductivity) and unpublished (permeability) studies on granular Fe_3O_4 – talc and Ni – talc wax systems. In these systems, plots of the real conductivity (σ'_m) against the volume fraction (φ) lie on a characteristic sigmoid curves that when fitted to the Two Exponent Phenomenological Percolation Equation (TEPPE), confirm the existence of “percolation microstructures” with critical volume fractions (φ_c). The plots of the real and imaginary permeability (μ'_m) and (μ''_m), satisfactorily fit to the TEPPE using the φ_c obtained in each case from the “conductivity” measurements. In all three cases, the conductivity results gave the exponent $t > 2$, and the permeability results gave $t < 1$.

Introduction: A theoretical understanding of the physical properties, being the complex conductivity (σ), complex dielectric constant (ϵ), complex permeability (μ), thermal conductivity (κ), and diffusivity (D) of various binary composites in relation to the volume fraction φ and topology of each component is of fundamental and practical interest. Published analytical expressions for these properties have evolved from early mixing rules¹⁻³ through Effective Media Theories (EMT)¹⁻³ and later percolation models^{4,5}. The Single Exponent Phenomenological Percolation Equation (SEPPE or GEM)³ was first derived and published in 1986, and is still in current use. The Two Exponent Phenomenological Percolation Equation^{6,7} (TEPPE), first published in 1997, reduces to the percolation equations^{4,5} in the limits where φ approaches 0 and 1, and also when φ is close to φ_c . In the present work, new DC and low frequency permeability data are fitted to the TEPPE, and the percolation exponents s and t were obtained (using both SEPPE (GEM) and TEPPE). Similar data which previously appeared in a thesis⁸ was also analysed. By usual convention, the volume fraction of the component with the higher value of the property of interest was explicitly expressed and was designated by φ .

Plots of $\log \sigma$ (or ε , κ , D or μ) versus φ for percolation systems are characterised by a sigmoid shaped curve. A rapid change in $\log \sigma$ (or ε , κ , D or μ) occurs at the critical volume fraction (percolation threshold) φ_c when the ratio of the properties of the two components is very large (i.e. $>10^6$). As the ratio of σ (or ε , κ , D or μ) decreases, the sigmoid shape slowly vanishes. The curvature in the regimes below and above φ_c are characterized, in fitting to TEPPE, by the exponents s and t , respectively. An adequate fit to certain data is sometimes also possible using the single component t in the SEPPE, where $s = t$.

Most of the TEPPE-derived parameters, s and t , are from electrical conductivity percolation experiments, which the literature shows to be the most commonly investigated percolation systems. Computer calculations⁵ for 3-D two component random composites of good and bad electrical conductors yield $t = 2.0$ and $s = 0.76$ as universal exponents for DC measurements. Several other theories⁵ for non-lattice solid state systems also yield $t > 2$. These give $t = 2.0$ and $s = 0.76$ as the universal exponents for DC conductivity measurements⁵. The Links-Nodes-Blobs model^{5,9-11} gives $t \geq 1 + (d-2) \gamma$, where d is the dimensionality of the system, and γ is the exponent in the equation for the average distance between the nodes in the percolation path. With $d = 3$ and $\gamma = 0.89$; this gives $t \geq 1.89$.

Pressed pellet systems, where the high conductivity and/or permeability component consists of grains with sharp edges and corners, are referred to as granular systems. Such systems contain a large number of point contacts between the high conductivity and/or permeability grains.

Experimental conductivity results^{6-8,12-17}, made on granular 3D systems, suggest that the lowest value of t from 3D experimental conductivity results¹⁴ may be 1.5. While most systems give $2 < t < 3$, some granular systems¹⁴ give t values as high as 5.25. There is only one reliable reported value for $t < 1$ in conductivity systems¹⁸. However, analysis¹⁹ shows that this is due to how the carbon nanotube structure evolves with φ . Based on the available evidence, it can be concluded that for simple percolation systems, which include granular ones, t is never less than 1 in conductivity systems.

Previous work on magnetic systems include measurements on sintered porous nickel of the real components of μ'_m , σ'_m and κ'_m made above φ_c in vacuo²⁰. These data were fitted with the SEPPE (GEM), using the same critical volume fraction $\varphi_c = 0.048$ and exponent $t = 1.9$. Other measurements²¹ of μ'_m , above φ_c where made on demagnetized Tungsten-Cobalt (WC grains coated and bound together by Co layers), were also fitted with SEPPE, and also yielded a $t < 1$. In all the measurements above the samples were demagnetized before each measurement.

Various studies on the permeability in magnetic (conducting) – non-magnetic (insulator) system at micro-wave frequencies have been published. Of these, only results of Chen et al.^{22,23} on a system of carbonyl iron powders (CIP) embedded in epoxy, were analysed using the TEPPE, and were found to fit the Bruggeman Symmetric Media Equation equally well³. The parameters given²³ are $\varphi_c = 0.333$ and $s \approx t \approx 1$. References [22] and [23] include references on the use of magnetic – non-magnetic composites in electronic engineering applications.

The new system studied in this paper consists of a binary mix of granular, paramagnetic and weakly electrically conducting Gadolinium Gallium Garnet (GGG: 0.3 to 26 Vol. %) and insulating and non-magnetic Teflon (PTFE) powder, on which conductivity and permeability measurements were made. Analysis of the data is presented and discussed together with permeability data, previously published only in a thesis⁸, on granular Fe_3O_4 – talc wax and Ni–talc wax systems. For these systems the fitting to TEPPE to the permeability data⁸ yields, $t < 1$ and for the conductivity data^{8,14} $t > 1$. This is a new observation and it is not yet known if there is a correlation between the permeability and conductivity results. To the author's knowledge, these are the first permeability results to be published for composite pressed pellets such as those used in conductivity measurements.

Theory: In this paper, $\sigma_m = \sigma'_m + i\sigma''_m$ ($\mu_m = \mu'_m + i\mu''_m$) is the composite conductivity (permeability), and the conducting (highly magnetic) component conductivity is $\sigma_h = \sigma'_h + i\sigma''_h$ ($\mu_h = \mu'_h + i\mu''_h$). For the insulating (non-magnetic or low conductivity) component it is $\sigma_i = \sigma'_i + i\sigma''_i$ ($\mu_i = \mu'_i + i\mu''_i$).

The TEPPE is a parameterisation of the BSME^{1,3} or the equivalent Symmetric Media Approximation (SMA) (Landauer^{2,24}). Both the BSME and SMA equations were derived from Maxwell's equations, for specific microstructures (Figure 1 and also see reference¹⁷ and the illustrations therein). The BSME (SMA) equations were derived for an array of identically shaped conducting and non-conducting ellipsoids, where the axis of rotation of both components are aligned. The size or axis of both components extend over an "infinite" range. The components that form the media are illustrated for spheres in Figure 0. In these derivations¹⁻³ spheres or ellipsoids are mixed, filling the space completely with the desired value of φ .

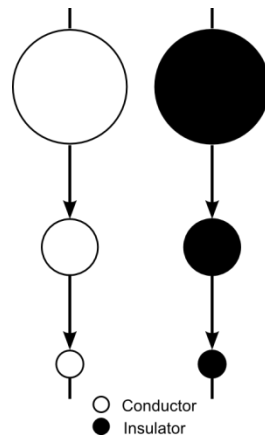


Figure 1. The Bruggeman Symmetric Media microstructure

The theoretical value of φ_c obtained for the space filling ellipsoids depends on the demagnetizing coefficient of the ellipsoids making up the media, and their orientation²⁵ with respect to the current (flux). In the TEPPE φ_c is a free parameter.

The TEPPE is given by:

$$(1-\varphi) (\sigma_l^{1/s} - \sigma_m^{1/s}) / (\sigma_l^{1/s} + A\sigma_m^{1/s}) + (\varphi) (\sigma_h^{1/t} - \sigma_m^{1/t}) / (\sigma_h^{1/t} + A\sigma_m^{1/t}) = 0, \quad (1)$$

With $A = (1 - \varphi_c) / \varphi_c$. The theoretical expression^{3,25} for A is $A = (1-L)/L$, where L is the demagnetisation coefficient of the spherical or ellipsoidal grains along the direction of the current or flux for that particular measurement. When $s = t = 1$, the above equation reduces to the BMSA or SMA equations. The frequency and temperature dependences resulting from the use of this equation are determined solely by the dispersive (and thermal²⁶) properties of both the components. Equation (1) yields the following:

$$\text{For } \sigma_h \rightarrow \infty: \quad \sigma_m = \sigma_l [\varphi_c / (\varphi_c - \varphi)]^s \text{ or } \mu_m = \mu_l [\varphi_c / (\varphi_c - \varphi)]^s. \quad \varphi < \varphi_c \quad (2)$$

$$\text{For } \sigma_l \rightarrow 0: \quad \sigma_m = \sigma_h [(\varphi - \varphi_c) / (1 - \varphi_c)]^t \text{ or } \mu_m = \mu_h [(\varphi - \varphi_c) / (1 - \varphi_c)]^t. \quad \varphi > \varphi_c \quad (3)$$

The cross over region^{4,5} occurs close to φ_c and lies between:

$$\varphi_c - (\sigma_l / \sigma_h)^{1/(t+s)} < \varphi_c < \varphi_c + (\sigma_l / \sigma_h)^{1/(t+s)}, \quad \varphi_c - (\mu_l / \mu_h)^{1/(t+s)} < \varphi_c < \varphi_c + (\mu_l / \mu_h)^{1/(t+s)}, \quad (4)$$

In the crossover region, the properties of both components contribute significantly to σ_m or μ_m . Equations (2) and (3) are the normalized standard percolation equations^{4,5} and characterize the exponents s and t . Most of the permeability results given here lie in the crossover region because, the values of μ_l / μ_h are significantly greater than zero. Only the TEPPE provides a continuous expression for the real components of σ , ϵ , κ , D or μ as a function of φ , from $\varphi = 0$ to 1. In some instances, a satisfactory fit to the experimental results can be obtained using the SEPPE (GEM), which is the TEPPE with $s = t$. If the same results are fitted with both the SEPPE and the TEPPE, the single parameter (t) obtained from the SEPPE is closer to the exponent t obtained from the TEPPE, both in magnitude and behaviour.

Kusy²⁷ has calculated the values of φ_c , for conductivity measurements, as a function of the ratio of the diameters of single sized insulating and single sized conducting spheres. Here φ_c corresponds to the situation where touching smaller conducting particles first coat the surface of the larger insulating particles with a 2D percolating network. A value of $\varphi_c = 0.03$ corresponds to a particle size ratio of 30. No such calculation has been reported for magnetic spheres, which would be needed to model permeability results. Obviously these particles do not have to touch in order to couple or interact.

Experimental: The granular ‘‘GGG’’ samples consisted of pressed pellets of thoroughly mixed ground Gadolinium Gallium Garnet (GGG: 0.3 to 26 vol. %) and free flowing Teflon (PTFE) powders. Stubby cylinders for permeability measurements (diameter 6 mm and 3-4 mm long) and discs (diameter 25 mm and 1.5- 2.5 mm thick) for conductivity measurements were pressed using hardened steel dies. The maximum pressures were approximately $300 \times 10^6 \text{ Kg/m}^2$ and $50 \times 10^6 \text{ Kg/m}^2$ for the stubby cylinders and discs, respectively. After pressing, both the stubby cylinders and discs were annealed at 280°C for 50 hours. The conductivity measurements were done at 250°C . Note that the samples for conductivity measurements reported in references [6 - 8] and [12 - 17] where made in similar manner.

The GGG powder was ground from off cuts of synthetic GGG platelets (Advanced Technology and Industrial Co. (Ltd), Hong Kong). A laser based size distribution analysis showed for the GGG that the peak volume frequency was at 22 μm , with 50 vol. % of the particles being smaller than 10 μm . For the Teflon powder the peak volume frequency was between 100 and 200 μm , with 50 vol. % of the particles being smaller 50 μm . Therefore near φ_c , most of the larger GGG particles should lie in the interstices formed by the still larger Teflon particles. The finer GGG particles (50% < 10 μm) coat the Teflon particles with a 2D conducting network which results²⁷ in a very low value for φ_c . The powders used to make each sample were mixed in the correct volume ratio using the mass and density of each component. The volume of the GGG in each sample was determined by the weight in the sample. This plus the measured volume of the sample enabled the volume fraction of the GGG to be determined. The volume of the Teflon includes the porosity. The electrical and magnetic properties of the starting GGG and Teflon used in this work were directly measured on the as-received materials.

Electrical conductivity of the GGG/Teflon samples was measured at 250⁰C using a Novocontrol Broadband Dielectric Converter (BDC) and Novotherm Temperature control system (Novocontrol Technologies GmbH & Co. KG, Germany). Isothermal static and complex susceptibilities at $H = 0$ and the saturation magnetization M_s ($B = 8.5$ T) were measured at 2K using a vibrating sample magnetometer (Cryogenic Ltd., UK) and an AC susceptibility system (Cryogenics Ltd, UK). The susceptibility (permeability) data have been corrected for a significant equipment related image effect against a niobium superconducting sample.

The preparation of the Fe_3O_4 – talc wax system and the Ni – talc wax system, and the electrical conductivity measurements with the results of fitting these results to the TEPE are described in references [8] and [14]. DC magnetic measurements were made using a vibrating sample magnetometer⁸. AC susceptibility measurements⁸ were made by passing the sample through two series apposed pick up coils in a 10 Hz 1 gauss AC field. The calibration of the system is described in reference [8].

Results and discussion: Figure 2 shows the experimental conductivity data, for the granular GGG systems, plotted as σ'_m against φ at 250⁰C. The line through the results is the best fit to Eq. 1, with the parameters: $\sigma'_l = 1.0002 \times 10^{-18}$ (S/cm), $\sigma'_h = 1.178 \times 10^{-12}$ (S/cm), $s = 0.8$, $t = 1.95$ and $\varphi_c = 0.05$. The fitted value of $\sigma'_h = 1.178 \times 10^{-12}$ S/cm agreed well with the value measured on a crystalline platelet of the as supplied GGG. As the values obtained for φ_c , s and t are typical for granular percolation systems¹⁴, it can be concluded that the GGG-Teflon system is a granular conducting percolation system. Here, coupling between grains occurs where the grains are touching, or close enough for the tunnelling of charge carriers. As previously stated, large numbers of point contacts between the sharp corners of the grains and their more planer surfaces characterize what are referred to, as granular systems. From Kusy's results²⁷, and the large ratio of the diameters characterizing the GGG and Teflon, a value of $\varphi_c \approx 0.05$ is expected.

The saturation magnetization M_s for the stubby cylinders and for a small single crystal ($\varphi = 1$) when plotted against calculated values for φ was found to vary linearly with φ . Thus,

interpolated values of $M_s(\varphi) / M_s(1)$ could have been used in place of the φ calculated from the volume fractions in the powders used to make each sample.

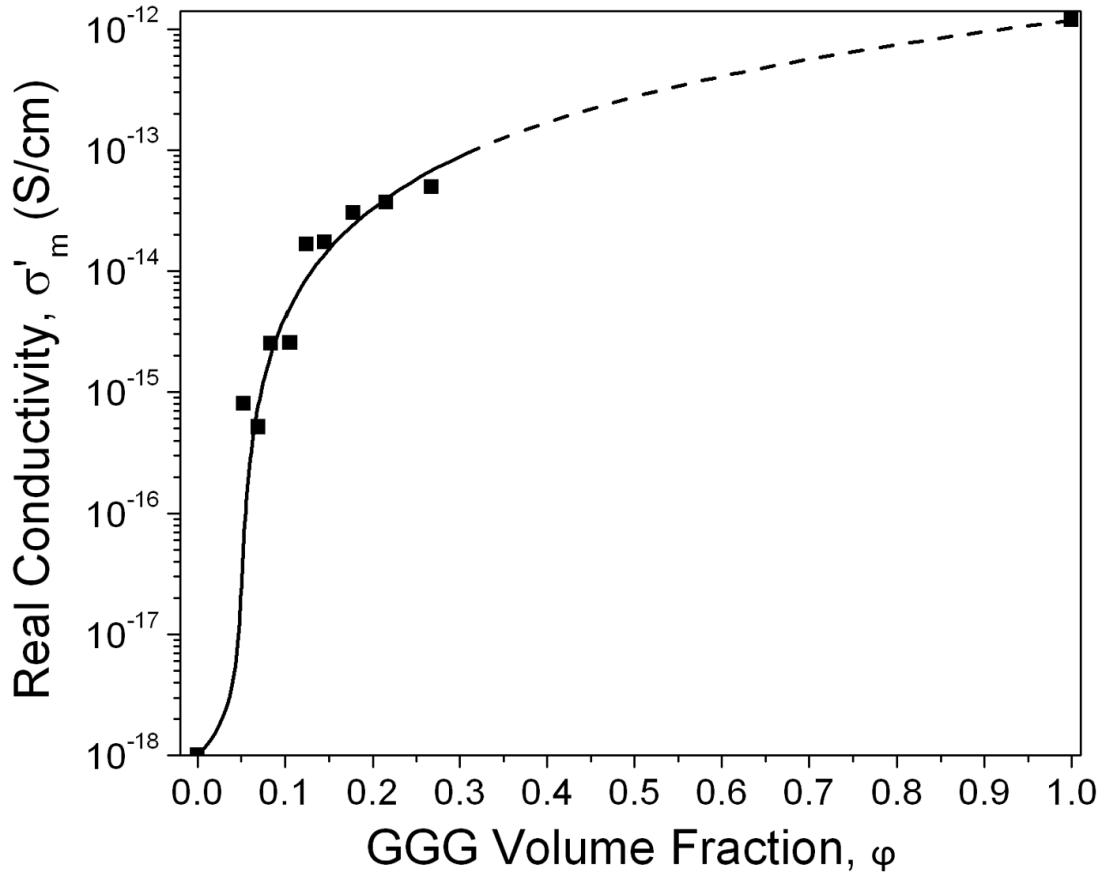


Figure 2. The experimental points, at 250 °C, for σ'_m , plotted against the GGG volume fraction, φ fitted to the TEPPE. The parameters are given in the text.

Figure 3 shows experimental data for the real permeability μ'_m against the volume fraction φ for various frequencies f , at $T = 2K$. Note that in fitting to this data, more consistent results were obtained with $s = t$. Best fits to the 0 Hz, 330 Hz and 2000 Hz data, using the SEPPE, are shown by the solid, dashed and dotted lines respectively. For all the fits to permeability data, given in tables 1 and 2, φ_c has been fixed at 0.05. With the best fit data (given in Tables 1 and 2), no significant improvement was found when φ_c was set as a free parameter. The real permeability for the Teflon (PTFE) was fixed at 1. (The volume fraction of the porosity is incorporated in the volume fraction of the Teflon, and also has $\mu'_1=1$). The final fixed values of t (real) and t (imag) and variable fitting parameters μ'_h and μ''_h used in Figs. 2 and 3 are given in Table 1. The procedure and justification used to arrive at the final parameters in Table 1 are outlined in the second paragraph below.

Freq. (Hz)	μ'_h	$\mu''_h \times 10^{-5}$	$\mu''_1 \times 10^{-6}$
0	4.39 ± 0.03	-	-
72	4.24 ± 0.02	1.93 ± 0.04	0.05 ± 0.06

330	4.19 ± 0.02	5.30 ± 0.40	1.00 ± 1.00
870	4.14 ± 0.03	9.20 ± 0.11	2.00 ± 0.70
2000	3.99 ± 0.02	13.9 ± 0.02	3.90 ± 0.30

Table 1: The SEPPE parameters used to plot the results in Figs. 3 and 4. $\varphi_c = 0.05$, t (real) = 0.432 and t (imag) = 0.757.

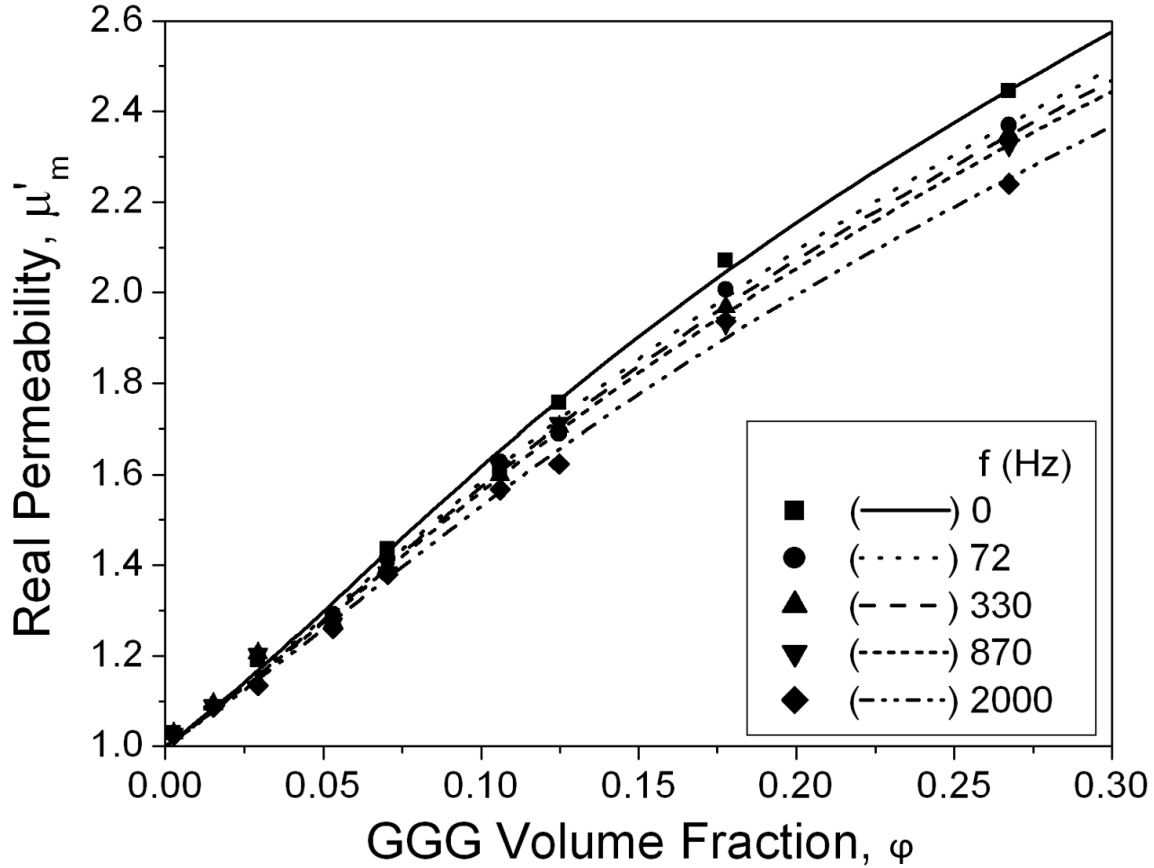


Figure 3 shows experimental data for the real permeability μ'_m against the GGG volume fraction φ for various frequencies f , at $T = 2K$. The best fits to the 0 Hz, 72 Hz, 330 Hz, 870 Hz and 2000 Hz data obtained using the SEPPE, are shown by the solid dashed and dotted lines respectively. The fitting parameters for this plot are given in the text and Table 1.

Figure 4 shows experimental data for the imaginary permeability μ''_m plotted against the volume fraction for various frequencies f , at $T = 2K$. The best fits to the data using the SEPPE, and the parameters in Table 1, are shown by the dashed lines. Again in fitting this data more consistent results were obtained with $s = t$. Best fits to the data using the SEPPE, the parameters given in Table 1, are shown in Fig. 4.

The parameters given in Table 1 were arrived at as follows. The data was fitted with φ_c fixed at 0.05 and μ'_1 fixed at 1.0. The results for the variable parameters obtained are given in Table 2. It can be observed that the values of t (real) are the same within the error, so it was fixed at the mean value (0.432) for all subsequent fittings. Without a theoretical or experimental suggestion of a frequency dependency of t ; the mean value of t (0.757) was used in the subsequent fitting of the imaginary data. These parameters are shown in Table

1. The fit in Figs. 3 and 4 are plotted using these parameters. Note that the values for t (real) are also less than 1, which is one of the most important insights gained from this research.

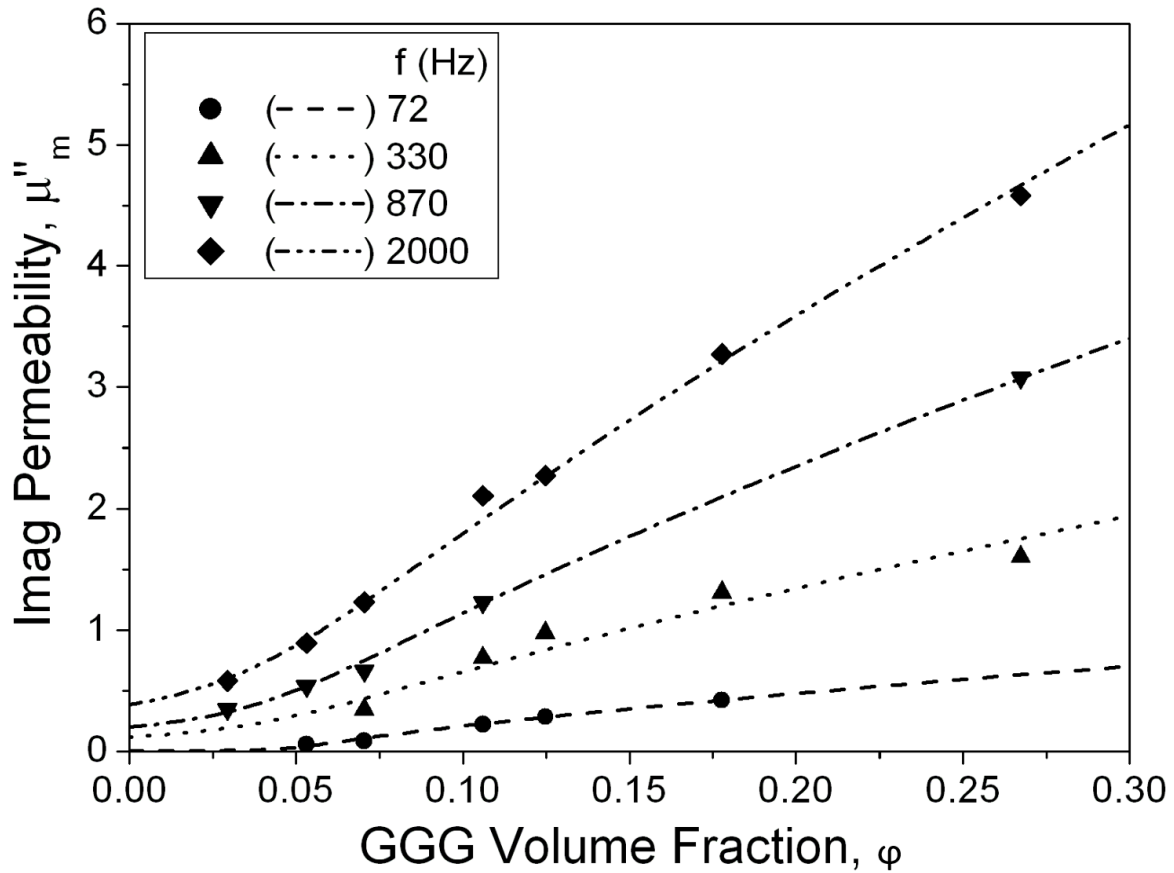


Figure 4 shows experimental data for the imaginary permeability μ''_m against the GGG volume fraction for various frequencies (f), at $T = 2K$. The best fit to 72 and 2000 Hz data using the SEPPE, is shown by the solid and dashed lines respectively. The fitting parameters for this plot are given in the text and Table 1.

Freq. (Hz)	μ'_h	t (real)	$\mu''_h \times 10^{-5}$	$\mu''_l \times 10^{-6}$	t (imag.)
0	4.5 ± 0.2	0.45 ± 0.40	-	-	-
72	4.3 ± 0.03	0.43 ± 0.03	2.2 ± 0.6	0.08 ± 0.07	0.81 ± 0.1
330	4.2 ± 0.2	0.44 ± 0.03	$3.4 \pm \text{inf}$	1.00 ± 1.00	$0.49 \pm \text{inf}^*$
870	4.1 ± 0.2	0.42 ± 0.04	11.0 ± 0.14	2.00 ± 0.70	0.79 ± 0.08
2000	4.0 ± 0.2	0.42 ± 0.04	12.1 ± 0.6	3.60 ± 0.30	0.67 ± 0.03

*Unstable fitting results not used in determining the mean values of t (imag).

Table 2 shows the results for the variable parameters when the data was fitted to the data with φ_c fixed at 0.05 and μ'_l fixed at 1.0 but may be greater than unity by such a small amount that it makes no difference to the fits for the real data.

GGG is a paramagnetic compound which obeys the Curie Law, and hence the susceptibility (permeability) depends inversely on the temperature. The real permeability μ'_m is determined by the number of freely rotating spins independent of any imperfections in the

GGG lattice. The imaginary permeability μ''_m depends on the damping of the spin rotation, which can depend on imperfections in the lattice, due to the prior grinding of the GGG. This can account for the different t values obtained from the real and imaginary results, or it could be due to inaccuracies in determining the values of μ'_h and μ''_h .

Earlier measurements^{8,14} of the conductivity and permeability of a Fe_3O_4 – talc wax system and a Ni – talc wax system, were made and analysed using the TEPPE. Plots of $\log \sigma_m$ against φ gave sigmoidal curves^{8,14}. These systems are similar to that shown in Fig. 2, which shows that these are percolation systems. The TEPPE conductivity parameters^{8,14} for the Fe_3O_4 – talc wax system were $\varphi_c = 0.025$, $t = 4.12$, $s = 0.45$, and for the Ni – talc wax system $\varphi_c = 0.025$, $t = 1.52$ and $s = 1.11$. Real permeability measurements on these systems were also made, and plots of μ'_m against φ , shown below in Figs 5 and 6 are similar to those in Fig 3. The TEPPE parameters for the Fe_3O_4 – talc wax system⁸ are $\varphi_c = 0.025$, $\mu'_h = 12$, $\mu'_l = 1$, $t = 0.53$, and $s = 0.45$ and for the Ni – talc wax system⁸ are $\varphi_c = 0.025$, $\mu'_h = 13$, $\mu'_l = 1$, $t = 0.52$, and $s = 1.11$. A larger value of μ'_h may account for the fact that the Fe_3O_4 – talc wax and Ni – talc wax systems can be fitted using the TEPPE. These results show the real and imaginary permeability data can be fitted with the same value of t when using the SEPPE (for the GGG-Teflon system), and separate s and t when using the TEPPE for the Fe_3O_4 – talc wax and the Ni – talc wax systems.

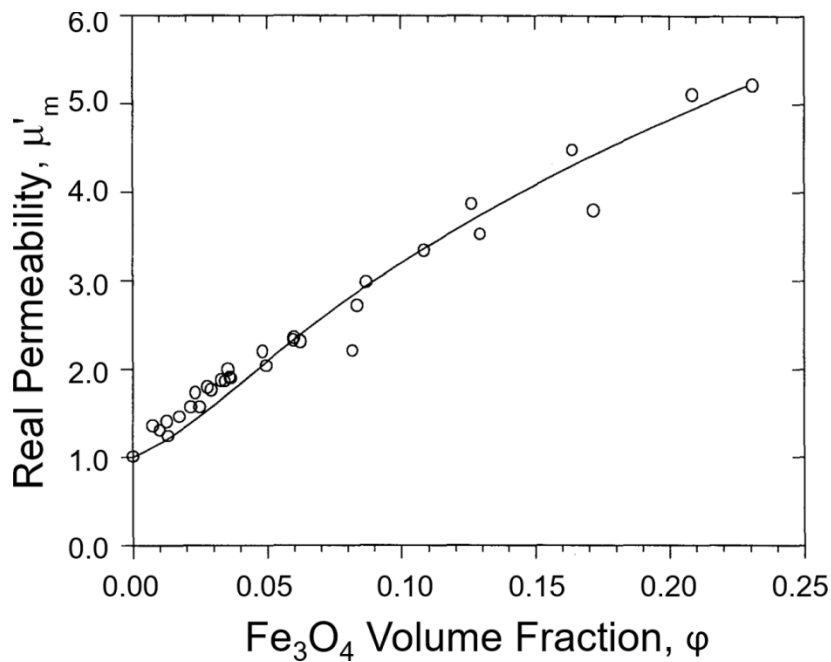


Figure 5. Permeability (μ'_m) plotted versus the Fe_3O_4 volume fraction (φ) for the Fe_3O_4 -Talc-wax samples⁸. The critical volume fraction from DC conductivity measurements for the system is; $\varphi_c = 0.025 \pm 0.003$. The solid line is a fit from eqn. (2.3), with the best-fit parameters; $\mu'_h = 12 \pm 3$, $\mu'_l = 1.00$, $t = 0.53 \pm 0.19$, $s = 0.45 \pm 0.31$ and $\varphi_c = 0.025 \pm 0.003$.

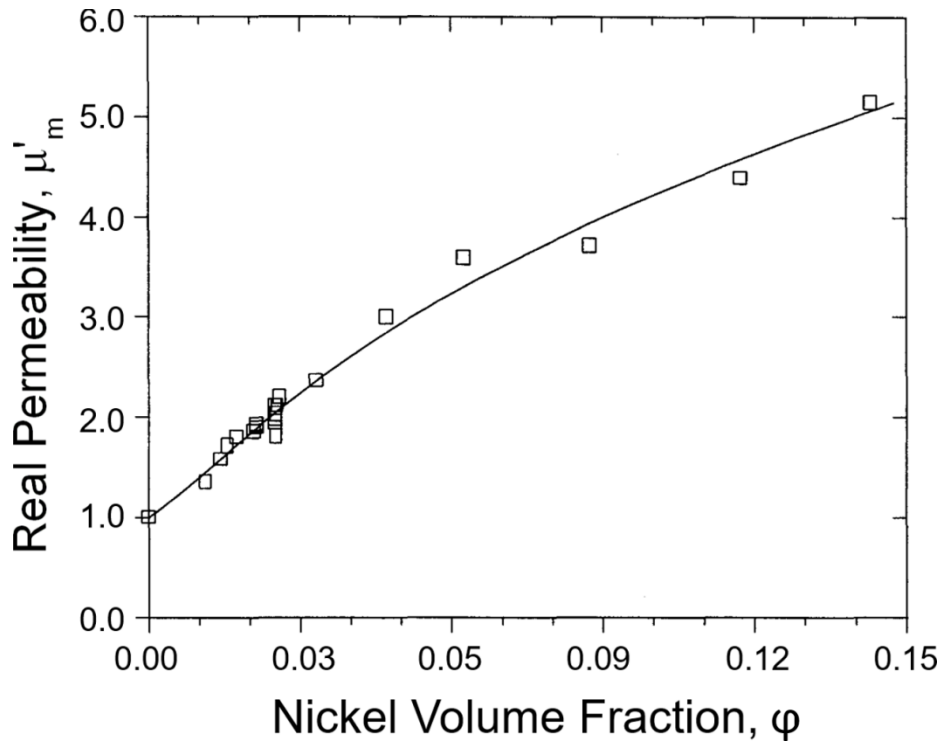


Figure 6, Permeability (μ'_m) plotted versus the nickel volume fraction (ϕ) for the Nickel Talc-wax samples⁸. The critical volume fraction from DC conductivity measurements for the system is; $\phi_c = 0.025 \pm 0.003$. The solid line is a fit from eqn. (2.3), with the best-fit parameters; $\mu'_h = 13 \pm 8$, $\mu'_l = 1.00$, $t = 0.52 \pm 0.46$, $s = 1.11 \pm 0.60$ and $\phi_c = 0.025 \pm 0.003$.

To appreciate these results, it must be realized that on a scale much larger than any of the grains in the sample, the sample is homogeneous. However, conductivity measurements show that on the scale of the grain sizes, the GGG grains form the current carrying Links-Nodes-Blobs model structure⁹⁻¹¹, characteristic of percolation systems. In the magnetic case, these links, nodes and clusters form paths of lower reluctance than the surrounding material.

The results from previous (1-9) and present measurements of the permeability of composites, fitted using the SEPPE (GEM) (1-9) or TEPPE (11 and 12), are given in Table 3 below. References for the previous measurements are given in the table. In general lower values of t seem to be obtained for the lower values of μ_h/μ_l .

	System	ϕ_c	μ_h/μ_l	t(s)	s
1	Coated Permalloy Flakes ²¹	1.0*	1287	21.5	-
2	Moly Coated Permalloy Flakes ²¹	1.0*	227	45	-
3	Mag. Balls in Brass powder ²¹	0.66	126	15.3	-
4	Iron Powder Mixed in grease ²¹	0.40	230	18	-
5	Carbonyl Iron ²¹	0.35	22.7	3.3	-
6	Mag. Cylinders in Brass powder ²¹	0.13	125	15.6	-
7	Cobalt coating TC grains (1) ²¹	0.133**	20.0	0.78	-
8	Cobalt coating TC grains (2) ²¹	0.088**	25.6	0.44	-
9	Sintered Nickel ²⁰	0.048	40.5	1.9	-
10	Gadolinium Gallium Garnet	0.05	4.5	0.432	-
11	Fe ₃ O ₄ – talc wax ⁸	0.025	12	0.41	0.45

12	Ni –talc wax ⁸	0.025	13	0.52	1.11
----	---------------------------	-------	----	------	------

*Fully coated flakes must have $\varphi_c = 1$ as the coating vanishes and the particles must touch.

** Cobalt is the binding component in TC-Co (hard metal).

Table 3. Parameters (with references) from previous measurements of the permeability of various composites, fitted using the SEPPE or TEPPE, are given in this Table.

Note for the systems in items 9 -12 above, the conductivity was measured and analysed using the TEPPE or SEPPE, which showed them to be conductivity percolation systems. The systems 1-6 are almost certainly also percolation systems. It should be noted that the t values are much higher than for conductivity systems^{6-8,12-17} which are typically 2-3 with a maximum of about 5.¹⁴ The systems 3, 4 and 5 are magnetic powders with no sharp edges or corners in a non-magnet matrix. At this time, it cannot be explained why values of t much higher than observed in conductivity measurements were seen in magnetic permeability.

As systems 10, 11 and 12 are granular systems, it would appear that when fitted to the TEPPE or SEPPE, give a t value less than 1. In systems 7 and 8, Cobalt was the binding component in TC-Co composite (hard metal) and has the form of convoluted sheets, with irregular shapes and cross-sections in the spaces between the TC grains. The convoluted sheets will make contact, at least close to φ_c through narrow necks on their peripheries. The nature of this sharply necked structure bears some resemblance to a granular structure. Except for the systems [10 – 12] presented in this paper, all other composite structures in the table give a t value greater than 1.

Conclusions: It has been shown that the TEPPE and/or the SEPPE can successfully model the permeability (μ) of magnetic - non-magnetic composites, as a function of the volume fraction φ . From these results there appear to be two classes of systems. The first is a granular magnetic particle system where the exponent t is less than 1. The second is one where the magnetic component is continuous or the grains make non granular contacts, and t is larger than 1. The fitting has been successfully made for both non – hysteretic systems (paramagnetic) GGG or hysteric systems. Although the imaginary permeability results μ_m'' have relatively large experimental errors in μ_h'' and μ_l'' , it can still be seen that the TEPPE can also fit the μ_m'' results.

This paper, along with previous referenced measurements in thermal conductivity and dielectric constants, show that t values < 1 occur only in systems with a granular structure. The occurrence and non-occurrence of t values < 1 , and also indicates the effect that the size distribution in the powders used to make the samples, will be dealt with in detail in a future paper³⁰. However, the complete understanding of the physical processes that determine the values of the exponents s and t remains to be theoretically established.

References

1. R. E. Meredith and C. W. Tobias, *Advances in Electrochemistry and Electrochemical Engineering* Vol 2, editor C W Tobias (Wiley-Interscience, New York) 1978,
2. R. Landauer, *American Institute of Physics Conference Proceedings* no 40, editors J C Garland and D B Tanner (American Institute of Physics) 1978.
3. D.S. McLachlan, M. Blaszkiewics, and R.E. Newnham, *J. Am. Ceram. Soc.* **73**, 2187 (1990).
4. J. P. Clerc, G. Girand, J. M. Langier, and J. M. Luck, *Adv. Phys.* **39**, 191 (1990).
5. D. J. Bergman, D. Stroud, *Solid State Physics* **46** (Academic Press, San Diego, 1992) p147.
6. Junjie Wu and D. S. McLachlan, *Phys.Rev.* **B56**, 1238 (1997).
7. Junjie Wu and D. S. McLachlan, *Phys. Rev.* **B58**, 14880(1998).
8. Cosmas Chiteme, *Thesis (University of the Witwatersrand)*. (2000)
9. H. E. Stanley, *J. Phys. A* **10**, L211 (1977).
10. A. Coniglio in *F.Disordered Systems and Localization* (Editors: Castellani, C., Di Castro, C. Peliti, (McMillian, Rome 1981). p 51. 25. H. E. Stanley, *J. Phys. A* **10**, L211 (1977).
11. D.Stauffer and A. Aharony, "Introduction to Percolation Theory, Second Edition," Taylor and Francis (1994).
12. D. S McLachlan, W. D. Heiss, C. Chiteme and Junjie Wu, *Phys. Rev.* **B58**, 13558 (1998).
13. W. D. Heiss, D. S. McLachlan and C. Chiteme, *Phys Rev.* **B62**, 4196 (2000).
14. C. Chiteme and D. S McLachlan, *Phys.Rev.* **B67**, 024206 (2003).
15. C. Chiteme, D. S. McLachlan and G. Sauti, *Phys.Rev.* **B75**, 094202 (2007)
16. D. S. McLachlan, G. Sauti C. Chiteme. *Phys.Rev.* **B76**, 014201 (2007).
17. D. S. McLachlan, *J. Electroceramics* **5**, 93 (2000).
18. W, Z. Shao et al., *J Phys: Cond. Matter* **20**, 39552 (2008).
19. I. Balberg, D. Azulay, Y. Goldstein and J. Jedrzejewski, *Phys. Rev.* **E93**, 062132 (2016)
20. N. Deprez, D. S. McLachlan and I. Sigalas, *Solid State Comm.* **66**, 869 (1988).
21. D. S. Mclachlan and H. White, *Journal of Magnetism and Magnetic Materials* **67**, 37 (1987).
22. Ping Chen et al., *J. Phys. D: Appl. Phys.* **38**, 2302 (2005).
23. Ping Chen et al., *J. Mag and Mag. Materials* **323**, 3081 (2016).
24. R. Landauer, *J. Appl. Phys.* **23**, 779 (1952).
25. F. Brouers, *J. Phys. C: Solid State Phys.* **C19** (1987).
26. D. S. McLachlan and M. B. Heaney, *Phys Rev* **B60**, 12746 (1999).
27. R. P. Kusy, *J. Appl. Phys* **48**, 5301 (1977).
28. B. Ghanbarian and H. Daigle, *Water Resources Research*, **52(1)**, 295 (2016).
29. D. S. McLachlan and Jie Chen, *J. Phys.: Condens. Matter* **4**, 4557 (1962).
30. D. S. McLachlan, T. B. Doyle and G. Sauti, *Private Communication*.